Bull. Mater. Sci., Vol. 17, No. 6, November 1994, pp. 893–910. © Printed in India.

Fractography as well as fatigue and fracture of 25 wt% silicon carbide whisker reinforced alumina ceramic composite

A K RAY, S BANERJEE*, E R FULLER -JR**, S K DAS† and G DAS†

MTE Division, †MTC Division, National Metallurgical Laboratory, Jamshedpur 831 007, India
*Research and Development Centre, SAIL, Ranchi 834 002, India
**Ceramic Division, National Institute of Standards and Technology, Gaithersburg, Maryland 20899, USA

Abstract. Fatigue cracked and fast fractured regions in four-point bend specimens prepared from 25 wt% silicon carbide whisker reinforced alumina composite were examined by scanning electron microscopy. This composite was found to be susceptible to a fatigue crack growth phenomenon similar to that in the case of metallic materials, but with a higher crack growth exponent. In the fatigue region, the alumina matrix failed mainly in a transgranular mode and the whiskers mainly failed with a flat fracture surface but without their pullout. On the other hand, in the fast fracture region, the whiskers failed predominantly by pullout and the alumina matrix failed in a mixed mode with about half in transgranular and the other half in intergranular mode. Thus, to improve the fracture toughness of the material, the grain boundary strength of alumina and the matrix whisker interfacial bonding should be improved. To increase the resistance to fatigue, the fracture strength of the alumina grains should be improved by using finer α-alumina particles and the fatigue strength of the whisker have to be increased by improving the uniformity in distribution of β-SiC whiskers during hot pressing.

Keywords. Alumina; silicon carbide; whiskers; fatigue; transgranular; intergranular; fracture strength.

1. Introduction

Fatigue crack growth rate (FCGR) (Ray and Banerjee 1994; Ray *et al* 1994) and fracture toughness (Krause and Fuller 1990; Ray and Banerjee 1994; Ray *et al* 1994) of 25 wt% silicon carbide whisker reinforced alumina ceramic composite have been studied and reported. Such studies are important since these materials have potential application in the production of structural components used at elevated temperatures, in high efficiency heat engines and heat recovery systems and for making cutting tools to machine special materials. When used in such applications, these ceramic components would often encounter monotonic and cyclic loading which produce crack extension. Therefore, the fractographic features of the fatigue failed samples need to be examined to identify the likely micromechanism of crack advance under monotonic and cyclic loading in this composite. Recently Dauskardt *et al* (1992) studied FCGR and made an extensive fractography of fatigue failed regions in a 15 vol% SiC whisker-reinforced alumina composite. The distinctly identified fractographic features at the low, medium, high ΔK (stress intensity range) fatigue region as well as in the fast fracture region can give clue to the likely mechanisms of fracture in our material.

2. Experimental procedure

The four-point bend specimens were sliced, prepared, surface finished and randomized from a 150 mm × 50 mm × 12·5 mm preformed billet of 25 wt% silicon carbide whisker reinforced alumina composite material (figure 1a). The details of fabrication of the billet is given elsewhere (Krause and Fuller 1990). The specimens in the

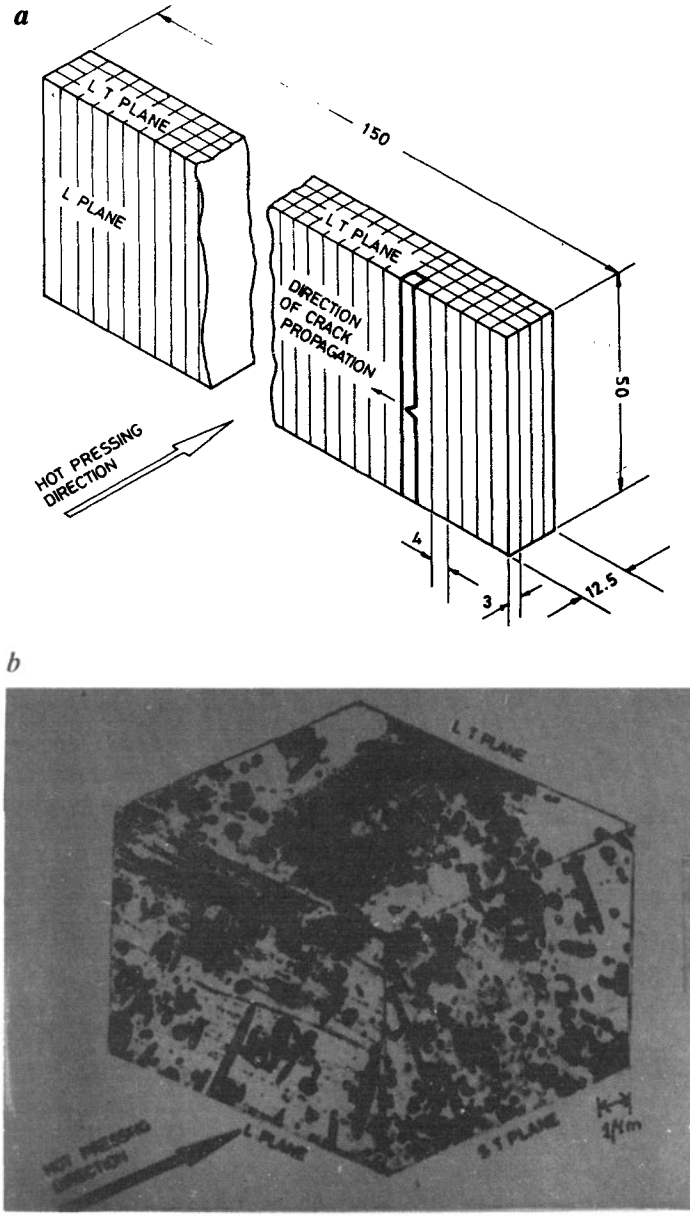

Figure 1. **a.** Billet prepared from the 25 wt% silicon carbide–alumina composite and **b.** montage of the microstructures shows distribution of SiC_w along the three planes.

present investigation were supplied to NML by the National Institute of Standards and Technology, USA.

The alumina powder used was of α-type (Krause and Fuller 1990; Ray *et al* 1994). The SiC whiskers had been produced in a carburization process at 1600°C where the sources of silicon and carbon were rice husk ash and rice husk hydrocarbons, respectively (Krause and Fuller 1990; Ray and Banerjee 1994).

The particle size of the alumina powder was less than 1 μm. Normal whisker diameter was 0·1 to 0·25 μm as revealed in the LT plane of the montage of the ceramic composite investigated here (figure 1b). The length of the whiskers varied between 10 to 30 μm (Krause and Fuller 1990).

The scanning electron microscopic (SEM) examination of the fracture surface of the specimens which failed due to premature crack extension during precracking in the conventional bridge fixture (Ray and Banerjee 1994; Ray *et al* 1994) showed that the alumina grain size after fabrication varied between 1 to 6 μm. This confirms that during hot pressing, the alumina underwent substantial grain coarsening, which, in areas where whiskers were absent or there was evidence of pores (figure 2), was as high as 6 μm. However, in other areas, the majority of the alumina grain size was in the range of 2 to 4 μm. This fracture surface indicated an intergranular fracture region in an otherwise transgranular region.

The montage of the ceramic composite revealed 3D-distribution pattern of the whiskers in the longitudinal (L), long transverse (LT) and short transverse (ST) planes. In the L plane, the whiskers appeared to be randomly oriented as the hot pressing direction is perpendicular to this L plane. During hot pressing, whiskers which are not normal to the L plane get further inclined thus producing the random orientation of the whiskers (Ray *et al* 1994). Since maximum material flow occurred along the LT planes during hot pressing, the whiskers get oriented normal to the

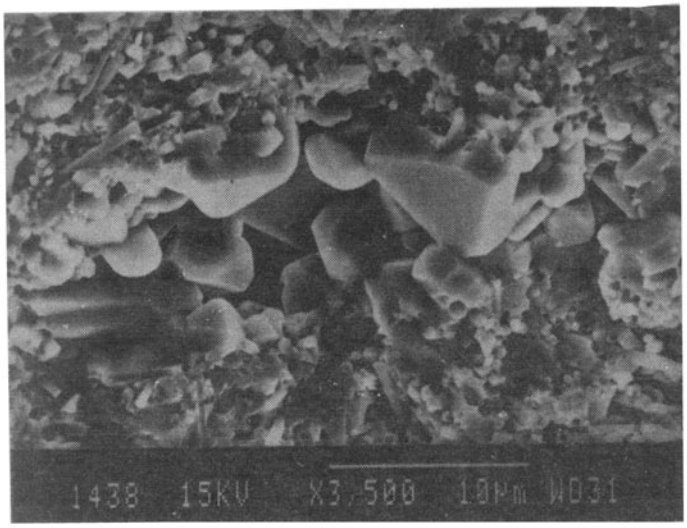

Figure 2. Fracture surface of the composite showing the size and shape of the alumina matrix.

LT plane. In the ST plane, there was a mixture of random orientation as well as normal alignment of the whiskers.

Becher and Wei (1984) concluded in their work that whisker orientation during processing of hot pressed SiC-whisker reinforced alumina leads to anisotropy in both fracture toughness and fracture strength of the composites. In other words, their fracture strengths are limited by the nonuniformity of the distribution of the whiskers i.e. by the ability to disperse the SiC whiskers. They also found that the dispersion of the whiskers improved by using finer alumina powder and hence an increase in the fracture strength of the composite was observed. Nevertheless, they have clearly observed (Becher and Wei 1984; Wei and Becher 1985) that similar to our composite under investigation (figure 1b), the whiskers are preferentially aligned perpendicular to the hot pressing axis. This type of distribution of whiskers suggested that a great deal of rearrangement of whiskers and powder occurred in the initial stage of densification of the composites and/or the matrix material underwent considerable deformation or creep during hot pressing.

The dimensions of the billet and the orientation of the four-point bend specimens (3 mm × 4 mm × 50 mm) in the billet is given in figure 1a. The 4 mm × 50 mm faces were normal to the hot-pressing direction so that both the directions of crack propagation (figure 3) and the crack plane were parallel to the LT plane (figure 1a) and normal to the hot-pressing direction (Krause and Fuller 1990). The 3 mm × 50 mm faces of the specimen were parallel to the ST plane.

A Vickers indentation produced at 0·8 kN load at the centre of the (3 mm × 50 mm) surface of the specimen acted as the crack starter on half of the four-point bend specimens. On the remaining half, notches were inserted exactly at the centre of the 3 mm × 50 mm surface of the specimens with a carborundum wheel to a depth of 0·1 mm. Thereafter, the specimens were subjected to fatigue loading in a servohydraulic test machine MTS-880 (100 kN capacity) to precrack the specimen in an articulated bridge fixture (Ray and Banerjee 1994), till the ratio of crack length to width was 0·05 on the (4 mm × 50 mm) surface of the specimen. Precracking was achieved with 100% success with the help of this fixture designed and fabricated at NML, Jamshedpur. Precracking was conducted at a force of 4 to 5 kN, load ratio, $R = 0{\cdot}1$ and frequency, $f = 20$ Hz. After this, the fatigue crack growth rate in the specimen was determined at increasing values of stress intensity range, ΔK (figure 4), under normal four-point bend loading (see figure 3) till the ratio of crack length to width was about 0·45–0·5, on the 4 mm × 50 mm surface of the specimen. Thereafter, the test to determine the fatigue crack growth rate was terminated and the specimen was subjected to monotonic loading to determine the fracture toughness of the material (Ray and Banerjee 1994) as per ASTM STP 410 (Brown and Srawley 1966). For both FCGR as well as fracture toughness (K_{IC}) tests, a 1 kN load range of the MTS-880 test machine was used. The test frequency was 1 Hz and the loading rate was 0·25 N S^{-1}. Tests were conducted in laboratory atmosphere and at ambient temperature. The fracture toughness testing produced fast fracture. The details of fracture toughness and FCGR tests are given elsewhere (Ray and Banerjee 1994; Ray *et al* 1994).

The fracture surfaces were coated with a thin film of gold (thickness 200°A) prior to SEM examination, in a JOEL JSM 840 A microscope.

The three regions viz. low ΔK corresponding to 0·8 to 1·8 MPa$\sqrt{m}$; high ΔK corresponding to 2·8 to 3 MPa$\sqrt{m}$; and, the fast fracture region corresponding to

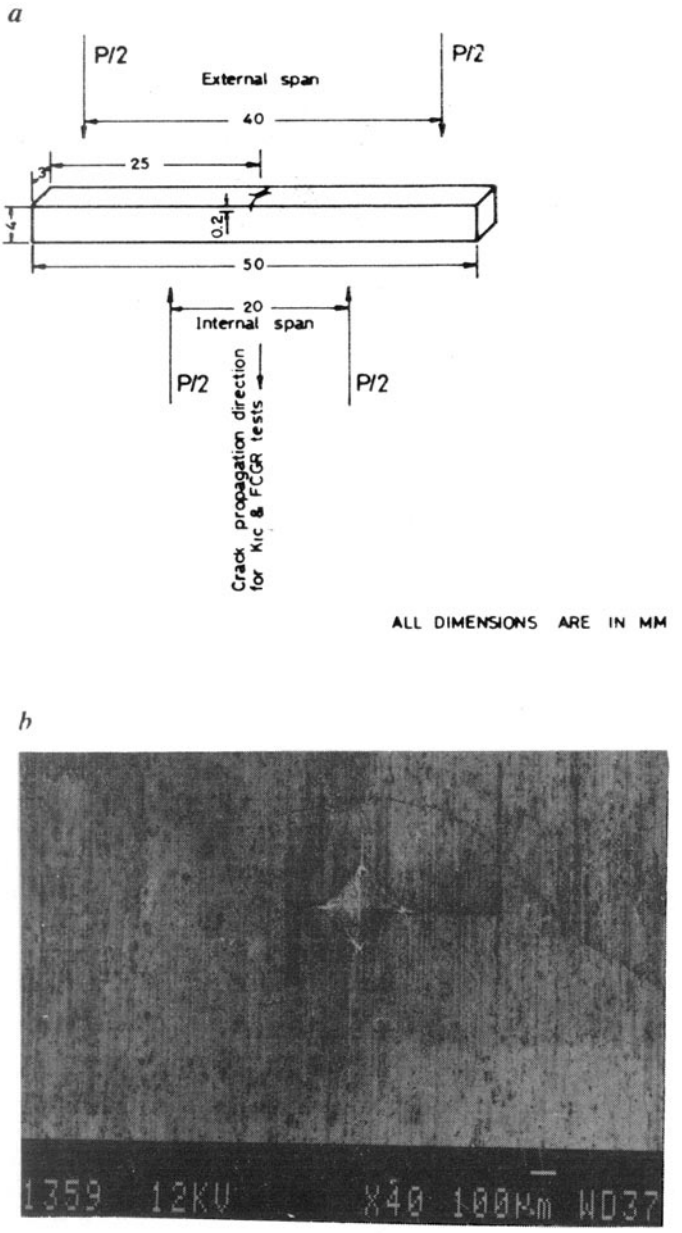

Figure 3. **a.** Indented and precracked specimen for four-point bend loading, and **b.** cracks are located at the four corners of indentation.

K_{IC} value of 5·9 MPa$\sqrt{m}$, were, at first, identified on the fracture surface at a magnification of ×30 under SEM (figure 5), using the details of the crack growth rate data generated on the specimen, as a guideline. The distinction between the fatigue and fast fracture could, however, be discerned through observation even

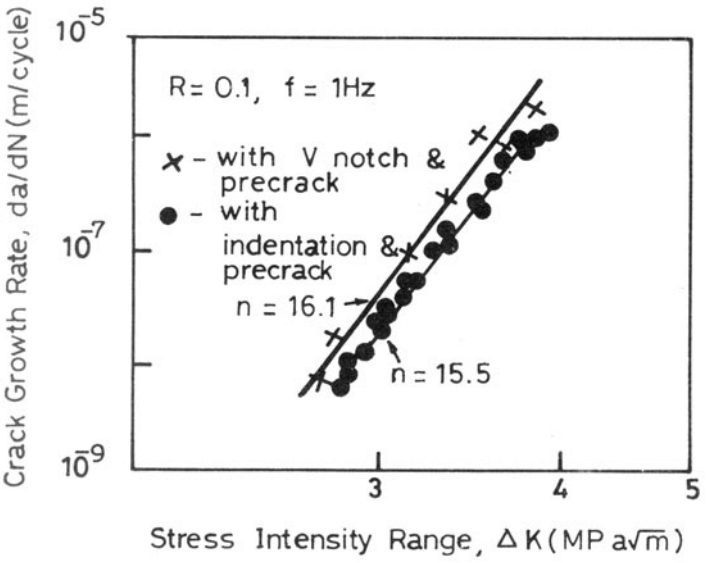

Figure 4. Fatigue crack growth data of 25 wt% SiC reinforced Al_2O_3 composite

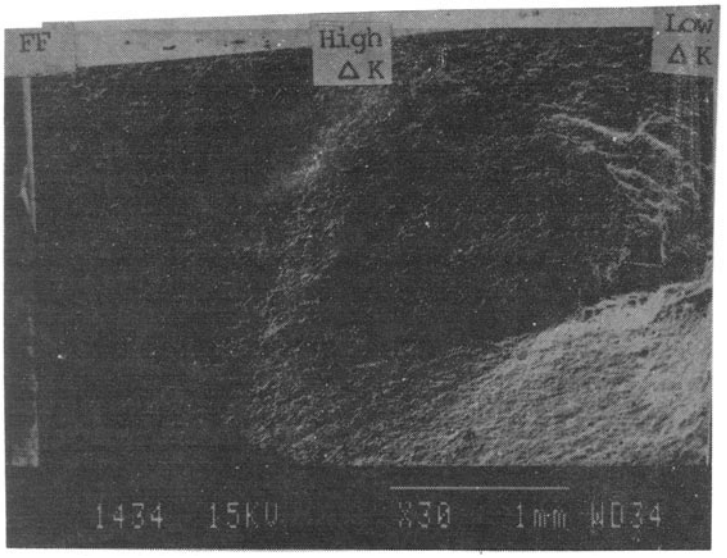

Figure 5. Entire fracture surface. (Right hand side, low ΔK region; middle, high ΔK region; left hand side, fast fracture region (FF)).

with the naked eye. The distinction between the low and the high ΔK fatigue regions was made from the crack length versus the number of cycles data generated during the fatigue loading of the specimen.

Each region was, at first, carefully scanned at low magnification, to identify the general and uniformly distributed features. Thereafter, it was examined at two

different magnifications ×4500 and ×7500, in order to identify the fractographic features and the mechanism of fracture in the low ΔK and the fast fracture regions.

3. Fractographic observations

A summary of the results of the fractographic observations is reported in table 1.

Table 1 states that, at low ΔK (0·8 to 1·8 MPa$\sqrt{m}$), the whiskers failed predominantly by shearing with a flat or square fracture without any visible evidence of necking; this was typical of fatigue fracture (figure 6). However, at high ΔK (2·8 to 3 MPa$\sqrt{m}$), the whisker failed in two different ways: i.e. about 60% of the whiskers failed with a flat fracture and the balance by pullout (figure 7). On the other hand, in the fast fracture region, the whiskers failed predominantly by pullout (figure 8).

Table 1 also reports that the matrix alumina grains failed predominantly through transgranular fracture (figure 9) at low ΔK (0·8 to 1·8 Mpa$\sqrt{m}$). In the high ΔK (2·8 to 3 MPa$\sqrt{m}$) region, the matrix failed in a mixed mode wherein about 45% of the alumina grains failed by intergranular and the balance by the transgranular mode, as shown in figure 10. During monotonic loading, the alumina grains in the fast fracture region also failed in a mixed mode with a slightly increased percentage of intergranular (~ 55%) and the balance by transgranular mode—as shown in figure 11.

It is noteworthy that in the low ΔK region, the crack had frequently branched (figure 12) and deflected (figure 13) while it propagated. Correspondingly, the river pattern markings with steps (figure 14) were also present in the cleavage facets. However, in the fast fracture region, the branching and deflection of the crack were virtually absent.

4. Discussion

Twentyfive weight percent silicon carbide whisker reinforced alumina composite is

Table 1. Fractographic features in the fatigue and fracture regions in a 25 wt% silicon carbide whisker reinforced alumina.

Mechanism of failure		Fatigue: low ΔK (0·8 to 1·8 MPa$\sqrt{m}$)	Fatigue: high ΔK (2·8 to 3·0 MPa$\sqrt{m}$)	Monotonic fracture (5·96 Mpa$\sqrt{m}$)
Whisker	Pullout (%) vs	5	40	85
	shear (%)	95	60	15
Matrix	Transgranular (%) vs	95	55	45
	intergranular (%)	5	45	55
Crack	o branching o deflection o river pattern	P	A	A

P, present; A, absent.

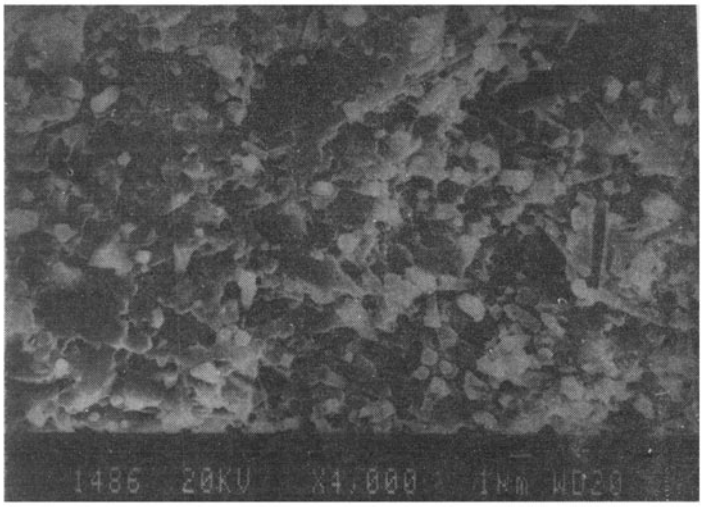

Figure 6. At low ΔK (0·8 to 1·8 Mpa$\sqrt{m}$) region, a majority of the whiskers failed with a square fracture without evidence of large scale pullout.

Figure 7. At high ΔK (2·8 to 3 MPa$\sqrt{m}$) region, the whiskers failed in a mixed mode, i.e. both with a square fracture and also by pullout.

susceptible to a fatigue crack growth phenomenon (Ray and Banerjee 1994; Ray *et al* 1994) as shown in figure 4, which is similar to that in the case of metallic materials, but with a higher crack growth exponent (n = 15·5 and 16·1). Figure 4 shows that the FCGR data of this material fits to the usual Paris equation

$$da/dN = A\,(\Delta K)^n.$$

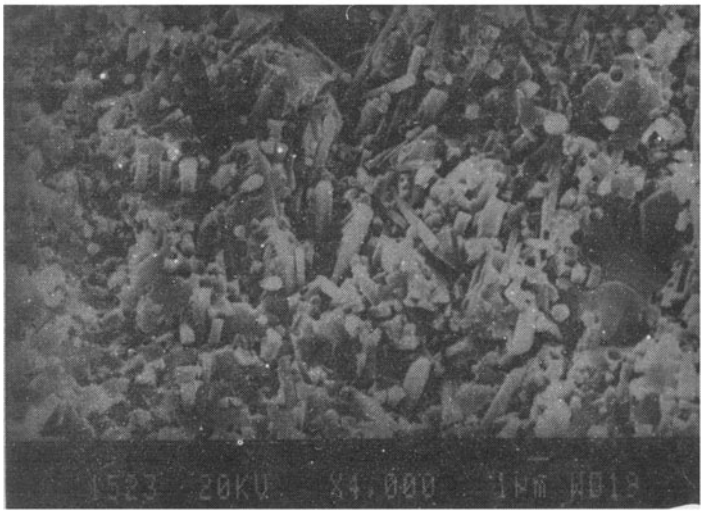

Figure 8. In the fast fracture region ($K_{IC} = 5{\cdot}9$ MPa$\sqrt{m}$), whiskers failed predominantly by pullout mechanism.

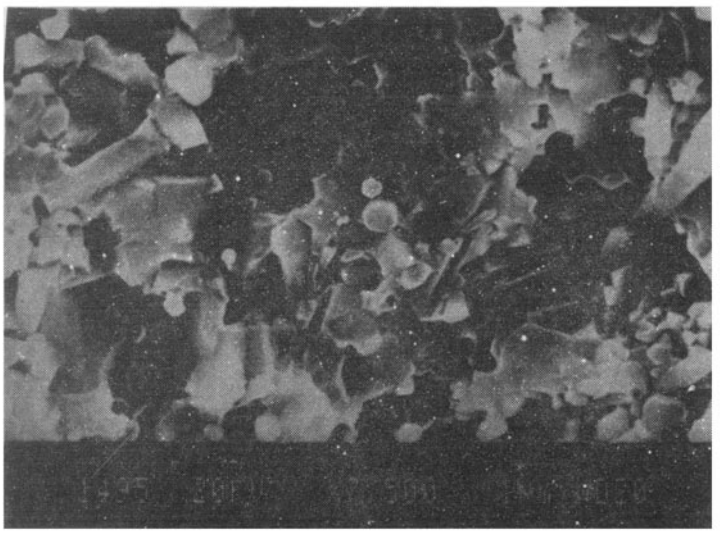

Figure 9. At low ΔK region, the alumina matrix failed predominantly through transgranular fracture.

Recently, FCGR data of 15 volume percent silicon carbide Al_2O_3 ceramic composite has been reported by Dauskardt *et al* (1992) using CT (compact tension) specimens. Comparison of FCGR data of these two composites with different whisker volume and porosity contents have been made and discussed elsewhere (Ray *et al* 1994). The Vicker's indentation when used as a crack starter induces certain amount of

Figure 10. At high ΔK region, the alumina grains failed in a mixed mode i.e. intergranular (~ 45%) and transgranular (~ 55%).

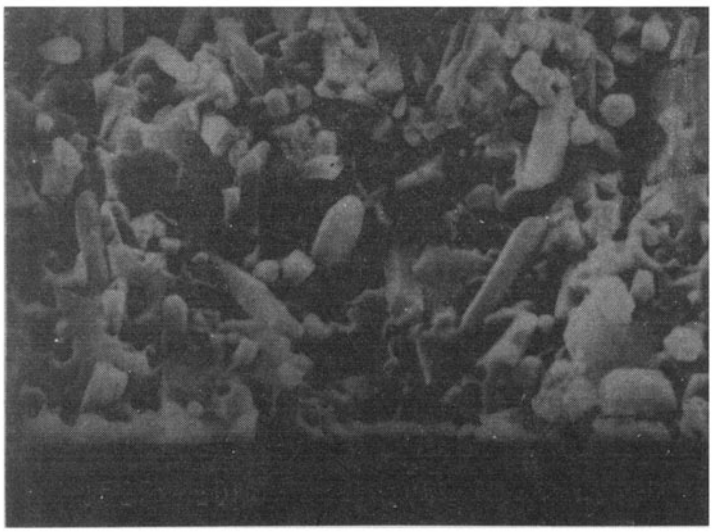

Figure 11. In the fast fracture region (monotonic loading), the alumina grains failed in a mixed mode, i.e. intergranular (~ 55%) and transgranular (~ 45%).

residual stresses in the material (Marshall and Lawn 1977; Ikuma and Virkar 1984; Ponton and Rawlings 1989). Residual stresses present in the parent sample due to grinding while fabrication and ahead of a V notch as well as indent along the crack propagation direction were determined using a X-ray stress analyzer, (AST-X2001). The details of residual stress measurement have been discussed

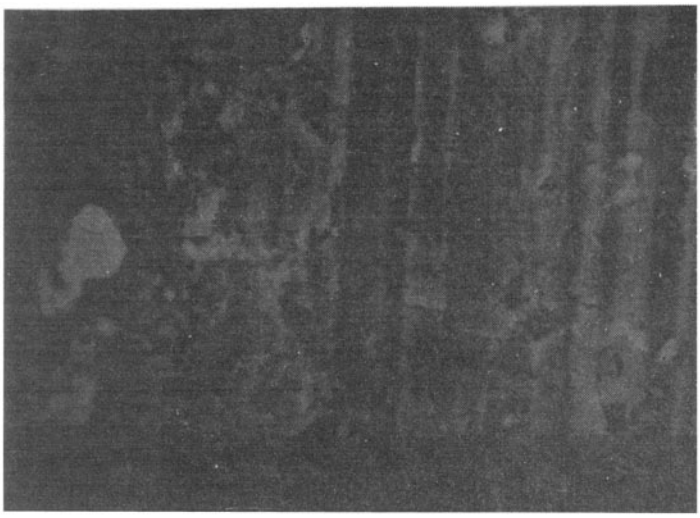

Figure 12. Crack branching in the low ΔK region.

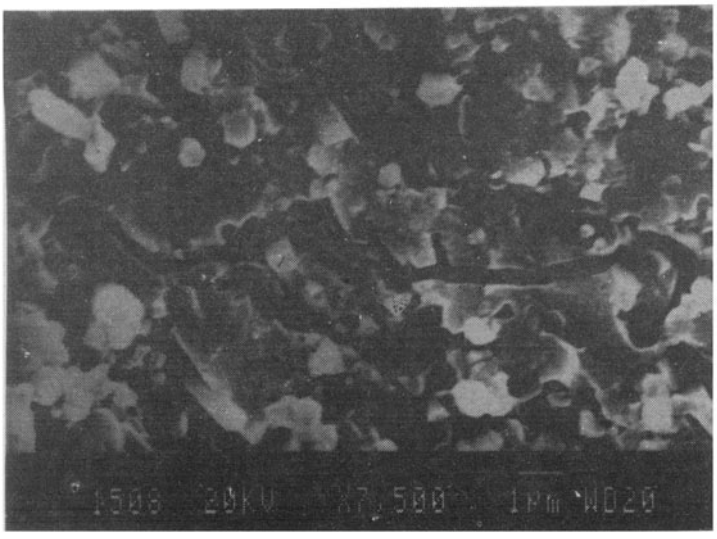

Figure 13. Crack deflection in the low ΔK region.

elsewhere (Ray and Banerjee 1994). If these stresses are compressive in nature, it would expect to retard the fatigue crack growth rate of the material. This type of behaviour was clearly demonstrated in our composite (figure 4), where the FCGR at a given ΔK for a V notch with precrack as a crack starter was slightly high compared to that in the case of indentation with precrack as a crack starter. Table 2 reveals that although the nature of residual stresses ahead of the advancing crack,

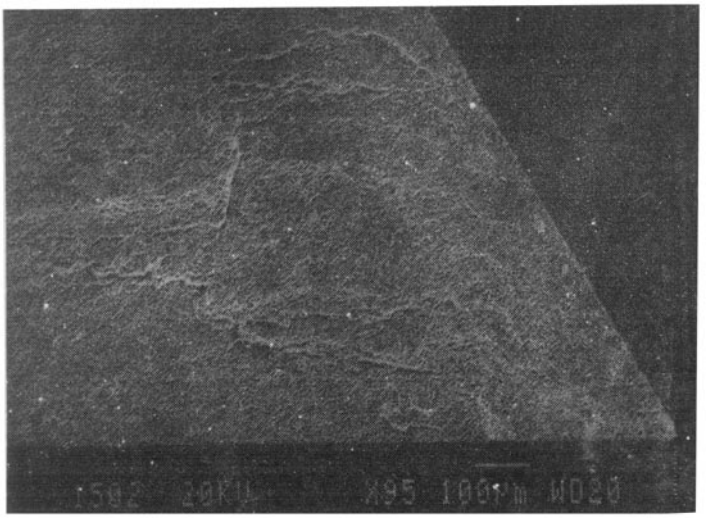

Figure 14. River pattern marking with steps in the low ΔK region (YZ, modulation SEM image).

Table 2. Residual stresses present in the ceramic composite.

Material	Specimen type	Residual stresses measured in AST-X 2001 (MPa)
25 wt% SiC reinforced Al_2O_3 ceramic composite	Parent	325·00 ± 0·4
	Ahead of indent	282·8 ± 0·8
	Ahead of notch	396·7 ± 0·9

were tensile for both notched and indented sample, relatively certain amount of compressive residual stresses were induced in the latter compared to the notched samples. The process of inserting a V notch in the specimen therefore has induced a considerable amount of tensile residual stresses. This is indicative of a higher n value (16·1) with a slight higher crack growth rate at a given ΔK in figure 4 compared to that of indented and precracked four-point bend specimen. The respective A values of Paris law equation have been given in table 3 (Ray and Banerjee 1994).

Fracture toughness values determined by using both types of crack starters and as reported in table 4 (Ray and Banerjee 1994), show that the average K_{IC} values obtained from indentation as a crack starter in indented and precracked specimens were ~ 7·77% higher than those obtained from V notched and precracked specimens. This possibly is attributed to the presence of less tensile residual stresses or in other words more compressive residual stresses in the notched sample compared to the residual stresses present in the indented sample, as can be confirmed from table 2. It should be noted that the term compressive is used only in a relative

Table 3. Paris law constants (A and n) from FCGR data.

Material	Type of specimen	A [m/cycle $(\text{MPa}\sqrt{m})^{-n}$]	N
25 wt% SiC reinforced Al_2O_3 ceramic	Notched and precracked	$5{\cdot}579 \times 10^{-16}$	16·1
	Indented and precracked	$3{\cdot}4 \times 10^{-15}$	15·5

Table 4. Fracture toughness K_{IC} determined by the ASTM procedure at NML.

	Fracture toughness K_{IC} in $\text{MPa}\sqrt{m}$		
	NML		NIST
Material	Notched and precracked	Indented and precracked	Indentation
25 wt% SiC reinforced Al_2O_3 ceramic composite	5·44	6·1	5·35 ± 0·17
	5·63	5·8	
	5·52	6·0	
	5·53 ± 0·05 average	5·96 ± 0·07 average	

sense in order to delineate from the tensile residual stresses already in the parent specimen as well as in the specimen with notch. The large difference in toughness between indented and precracked specimens (table 4) and the one reported by NIST, could primarily be accounted for the difference in crack tip loading rates. Fuller has represented K_R values from the expression

$$K_R = 5{\cdot}35\,(C/18{\cdot}1\ \mu\text{m})^{0{\cdot}08},$$

where C is the crack length and K_R is a parameter which describes the fracture resistance for a R-curve material. Using this relation one could derive an indentation-crack-length toughness (Krause and Fuller 1990). In R-curve type materials, the toughness varies with crack extension, so that if one attempts to measure the toughness with a procedure that ignores this as do most of the earlier indentation techniques, one would find that measured toughness depends on indentation loads.

Since the manner of failure of the whiskers and the α-alumina grains were entirely different in the low ΔK fatigue and the fast fracture regions, the scheme of crack growth under these two conditions are discussed separately, to focus on their contradistinctions.

4.1 *Low ΔK fatigue region*

During fatigue loading at the low ΔK regions, when $K_c = 1{\cdot}8$ to $2\ \text{MPa}\sqrt{m}$ – the alumina grains of the matrix failed mainly by transgranular cleavage with frequent crack branching and crack deflection. Also, the cleavage facets revealed river pattern

and steps. At low ΔK, the K_c values and consequently the traction force ahead of the crack tip, were not large enough to promote intergranular fracture.

At low ΔK, the amount of crack extension is very low. So even though the energy dissipated per cycle is low, the number of cycles and the cumulative energy required for a given amount of crack extension is quite significant and can thus account for the higher surface area required for the various features encountered like crack branching, river pattern and steps.

At low ΔK fatigue, the whisker could fail in three different modes: (i) pullout, (ii) tensile fracture and (iii) fatigue. Table 1 shows that only a few of the whiskers failed due to pullout at low ΔK fatigue. This naturally indicated that the maximum traction forces generated ahead of the crack tip during the low ΔK fatigue was not adequate to produce a pullout. Thus, it is likely that the whiskers continue to bridge the crack even after some of the surrounding alumina grains had failed by transgranular cleavage. Therefore, under these circumstances, the whisker could fail due to tensile fracture or fatigue.

One might rule out the possibility of tensile fracture if one had examined the relative values of strength and Young's modulus reported by Fisher *et al* (1991) and Ray *et al* (1991). The fracture strength of the whisker is about 6·5 to 7 times higher than that of alumina. Accordingly, the tensile fracture of the whisker was unlikely if the traction forces ahead of the crack tip were to be distributed in proportion to the relative cross-sections of the whisker and alumina in the plane of the crack. Even if the whiskers were to carry the major part of the traction forces ahead of the crack tip, the high traction forces would produce failure by pullout rather than by tensile fracture, as was observed in the fast fracture region where K_{IC} values and consequently the traction forces, were high.

Since the possibility of large scale failure by pullout or tensile fracture was discounted, whiskers were most likely to fail by fatigue. At low ΔK, the whiskers which had bridged the crack after the surrounding alumina grains had failed by cleavage, would continue to experience fatigue loading, then failed with a square fracture which is typical of fatigue. The fatigue failure of the silicon carbide whisker under such circumstances, could be significantly influenced by the stacking fault such as is reported in figure 15 (Ray *et al* 1991), since such fault could be responsible for nucleating the fatigue crack. However, this aspect needs careful study.

Since cleavage of the α-alumina grains occurred probably before the whiskers (located mainly at the grain boundaries) had failed, it was necessary to improve the fatigue resistance of the α-alumina grains. This apart, the dislocation pile-up model (Kingery *et al* 1976) would obviously indicate that the cleavage failure of α-alumina could be prevented through the refinement of alumina grains in the aggregate structure. The size of alumina grains varied between less than 1 to 6 μm. In this context, one should note that one could obtain higher resistance to low ΔK fatigue, if ultra-fine or nano-size alumina grains such as that produced by the sol-gel technique were to be used to fabricate this composite.

A schematic view of crack propagation mechanism is represented in figure 16a. It illustrates that at low ΔK fatigue, the matrix failed predominantly by transgranular fracture and the advancing crack frequently branched and tilted and twisted in its course of deflection. Since the whiskers were predominantly located at the grain boundaries and the crack propagation along the grain boundary at low ΔK fatigue

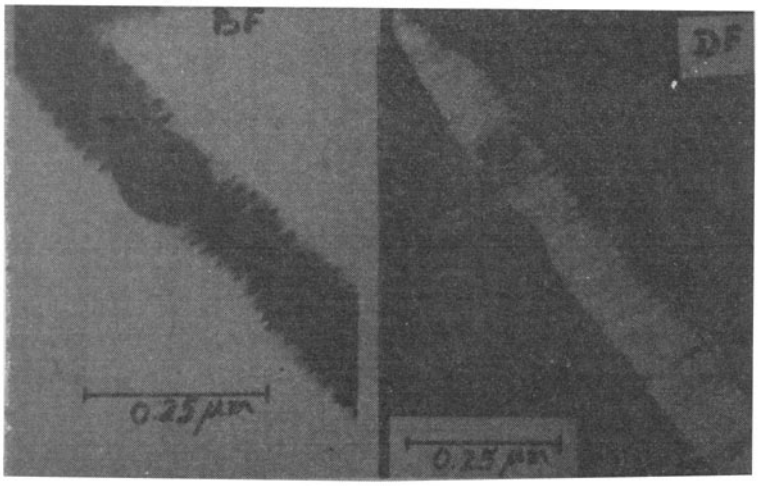

Figure 15. TEM of β-SiC whisker showing stacking fault by dark field and bright field techniques (Ray *et al* 1991).

was negligible, the possibility that the crack would encounter these whiskers as it advances would be rather low. Only a few of those whiskers which had bridged the crack with an orientation normal to the advancing crack plane, could fail by pullout. The other whiskers were likely to fail by directly experiencing fatigue loading. This could explain why at low ΔK fatigue, a majority of the whiskers failed with a square fracture and without pullout.

4.2 *Fast fracture region*

During the fast fracture under monotonic loading such as during the fracture toughness testing, some of the α-alumina grains of the matrix failed by intergranular fracture; the others failed by transgranular cleavage. The value of K_{IC} during such monotonic loading was 5·9 MPa$\sqrt{m}$. At such values of K_{IC}, the traction force generated ahead of the crack tip, was adequate to produce the intergranular failure in those grains which were favourably oriented with respect to the direction of the traction force. Debonding and pullout of those whiskers at the fractured grain boundaries would therefore occur.

It is difficult to summarize from the fractographic features as to which of these, i.e. transgranular cleavage or intergranular fracture occurred, at first, under monotonic loading.

After some of the grains had failed through the intergranular mode, the other neighbouring grains which were less favourably oriented or which were strongly anchored by the whiskers across the grain boundaries, failed through transgranular cleavage.

The pullout of the whiskers could be avoided if the whisker alumina interfacial strength was improved or if finer and more numerous whiskers and also finer α-alumina particles were used in fabricating the composite. Similarly, the intergranular fracture could be avoided by strengthening the boundaries.

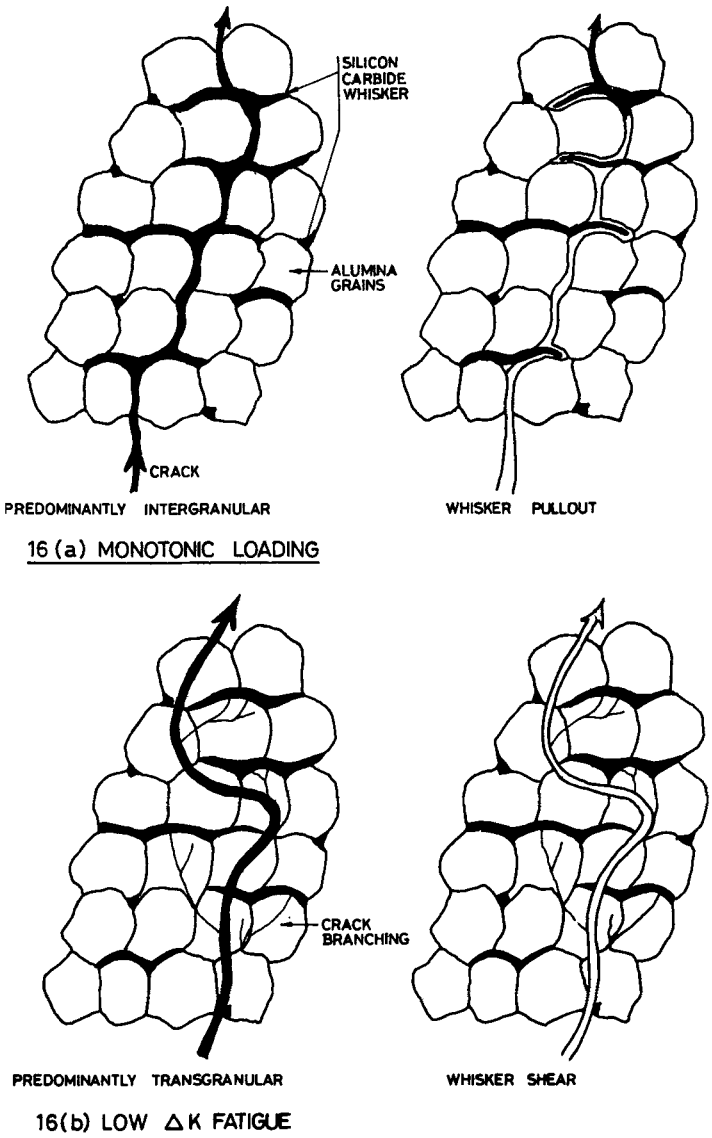

Figure 16. Schematic of the crack propagation during monotonic and cyclic loading.

As illustrated schematically in figure 16b, the fracture due to monotonic loading showed a substantial amount of intergranular failure of the matrix and pullout of the whiskers. Crack deflection, branching and the characteristic river pattern marking with steps, were absent in this region.

The matrix failure was predominantly intergranular. Nevertheless, the whiskers are located mainly at the grain boundaries. Therefore the probability of the advancing crack front interacting with the whiskers was extremely high. The whiskers tending to bridge the advancing crack quite frequently would therefore get debonded and pullout—which is schematically illustrated in figure 16b—were located at the grain boundaries only. Therefore, the whiskers would tend to bridge the advancing crack

quite frequently and, therefore, these would get pulled out which is schematically illustrated in figure 16b. This justifies the fact that during the monotonic fracture, failure of whiskers by the pullout mechanism was frequently observed in the fractograph.

During fatigue loading at high ΔK, mechanism of fracture was an intermediate situation between the two extreme cases, i.e. between the monotonic fast fracture and that of the low ΔK fatigue fracture.

Since the ceramic material is often expected to survive both monotonic and fatigue loading, one could make the following general observations based on the scheme of crack growth under the two conditions as discussed above.

To prevent fracture failure of this ceramic material under monotonic loading, its microstructural features would have to be strengthened to avoid intergranular fracture of α-alumina and the pullout of the whisker. This requires that the grain boundary strength of α-alumina and the whisker-matrix interfacial strength should be increased. Similarly, to retard crack extension during low ΔK fatigue, intergranular cleavage fracture of α-alumina grains and fatigue failure resistance of the silicon carbide whiskers should be improved, possibly by using finer α-alumina powder (Becher and Wei 1984; Wei and Becher 1985) and by improving the uniformity of distribution of whiskers in the matrix during hot pressing (Becher and Wei 1984, 1985) of the whiskers.

5. Conclusions

The following conclusions were arrived at from the results of this study.

(i) 25 wt% SiC reinforced Al_2O_3 ceramic composites are susceptible to a crack growth phenomenon which is similar to that in the case of metallic materials but with a higher exponent.

(ii) There was 100% success in pre-cracking ceramic specimens with the help of an articulated bridge fixture. Between indented with precrack and V notched with precrack four-point bend specimens, the use of indentation as a crack starter influenced the K_{IC} values mainly and the fatigue crack growth rate to some extent, due to the presence of certain amount of compressive residual stresses ahead of the advancing crack.

(iii) The micro-mechanism of fracture of a 25 wt% silicon carbide whisker reinforced alumina composite when loaded in fatigue was quite different from that when loaded monotonically. Consequently, the fractographic features in the two instances of loading were significantly different.

(iv) When loaded in fatigue, the alumina matrix failed in a transgranular mode and the whiskers failed by producing a flat fracture but without their pullout.

(v) When loaded monotonically, the whiskers predominantly failed by pullout and the alumina matrix failed in a mixed mode with about half in transgranular and the other half in intergranular mode. Whereas the grain boundary strength of α-alumina and the whisker-matrix interfacial bonding should be increased to produce increased resistance to failure under monotonic loading. The fatigue failure resistance could be improved by improving the cleavage strength of the α-alumina grains i.e. by using finer α-alumina particles and by increasing the fatigue strength of the whiskers by improving the uniformity in the distribution of β-SiC whiskers during hot pressing.

Acknowledgements

The authors gratefully acknowledge the help and advice of Mr N K Das and Prof. O N Mohanty in the SEM work. The authors are thankful to Dr D K Bhattacharya and Dr (Mrs) Aruna Bahadur for their assistance in measuring residual stresses.

References

Becher P F and Wei G C 1984 *J. Am. Ceram. Soc.* **67** 267
Brown W F Jr and Srawley J E 1966 ASTM-STP-410 (Philadelphia: ASTM)
Cook J L and Rhodes J R 1986 *88th Annual meeting of the American Ceramic Society, Chicago, IL*
Dauskardt R H, Porter J R and Ritchie R O 1992 *J. Am. Ceram. Soc.* **75** 759
Fisher E S, Manghnani M H and Routbort J L 1991 *Study of the elastic properties of Al_2O_3 and Si_3N_4 material component, high performance composites for the 1990s* (eds) S K Das, C P Ballard and F Marikar (The Minerals, Metals and Materials Society) p. 365
Ikuma Y and Virkar A V 1984 *J. Mater. Sci.* **19** 2223
Kingery W D, Bowen H K and Uhlmann D R 1976 *Introduction of ceramics* (New York : John Wiley and Sons, Inc.) 2nd ed. p. 795
Krause R F Jr and Fuller E R Jr 1990 *J. Am. Ceram. Soc.* **73** 559
Marshall D B and Lawn B R 1977 *J. Am. Ceram. Soc.* **60** 86
Ponton C B and Rawlings R D 1989 *Br. Ceram. Trans. J.* **88** 83
Ray A K and Banerjee S 1994 *J. Am. Ceram. Soc.* (accepted)
Ray A K, Fuller E R and Banerjee S 1994 *J. Eur. Ceram. Soc.* (accepted)
Ray A K, Mohanty G and Ghosh A 1991 *J. Mater. Sci. Lett.* **10** 227
Wei G C and Becher P F 1985 *J. Am. Ceram. Soc. Bull.* **64** 298